

COLLIMATION OF HEAVY-ION BEAMS IN THE HE-LHC*

A. Abramov^{1,2†}, R. Bruce², M. Crouch², N. Fuster-Martinez²,
A. Mereghetti², J. Molson², L. J. Nevay^{1,2}, S. Redaelli²

¹John Adams Institute at Royal Holloway University of London, Egham, TW20 0EX, UK

²CERN, 1211 Geneva 23, Switzerland

Abstract

A design study for a future collider to be built in the LHC tunnel, the High-Energy Large Hadron Collider (HE-LHC), has been launched as part of the Future Circular Collider (FCC) study at CERN. It would provide proton collisions at a centre-of-mass energy of 27 TeV as well as collisions of heavy ions at the equivalent magnetic rigidity. HE-LHC is being designed under the stringent constraint of using the existing tunnel and therefore the resulting lattice and optics differ in layout and phase advance from the LHC. It is necessary to evaluate the performance of the collimation system for ion beams in HE-LHC in addition to proton beams. In the case of ion beams, the fragmentation and electromagnetic dissociation that relativistic heavy ions can undergo in collimators, as well as the unprecedented energy per nucleon of the HE-LHC, requires dedicated simulations. Results from a study of collimation efficiency for the nominal lead ion ($^{208}\text{Pb}^{82+}$) beams performed with the SixTrack-FLUKA coupling framework are presented. These include loss maps with comparison against an estimated quench limit as well as detailed considerations of loss spikes in the superconducting aperture for critical sections of the machine such as the dispersion suppressors.

INTRODUCTION

The High-Energy Large Hadron Collider (HE-LHC) is a design study for a future energy frontier proton-proton collider with 27 TeV centre-of-mass energy [1–4]. The HE-LHC will use the magnet technology proposed for the hadron option of the Future Circular Collider (FCC-hh), but will be housed within the existing LHC tunnel. Because of the tight space constraints, the optics and layout of the lattice in some regions differ from those of the LHC. A multi-stage collimation system is foreseen in the HE-LHC. Apart from protecting the machine from regular and irregular betatron losses, which is the main focus of this work, the collimation system should also provide machine protection [5] and minimise experimental backgrounds [6, 7]. Although the collimation system design is based on that of the LHC [8, 9] and HL-LHC [10, 11], there are some key differences. As in the LHC, collimators are housed in two dedicated insertion regions (IRs) i.e. IR7 for betatron collimation and IR3 for off-momentum collimation. Each of these IRs in-

cludes a 3-stage collimation system - primary collimators (TCPs) intercept halo particles, secondary collimators (TC-SGs) capture particles out-scattered by the TCPs and shower absorbers (TCLAs) stop the showers generated in collimators upstream. Additional collimators are installed around the experimental insertions.

Thanks to the experience gained during the HL-LHC study [12], dispersion suppressor collimators (TCLDs) were also foreseen early on in the HE-LHC design process to protect the dispersion suppressor (DS) of the betatron collimation insertion from off-momentum losses coming from the warm straight sections. In the HE-LHC, the space for the TCLDs is achieved by optimising the layout in the DS [13] rather than replacing main dipoles in the DS by shorter and stronger magnets like in the HL-LHC. The betatron collimation insertion, including 2 TCLDs, has been successfully integrated into the lattice, but the impact on collimation cleaning efficiency must be carefully assessed.

With a total stored beam energy of almost 50 MJ, about a factor 4 beyond what has been achieved operationally with Pb ion beams in the LHC [14], Pb collimation becomes extremely challenging in the HE-LHC. Regular beam losses are unavoidable, and the superconducting magnets are very sensitive to any local losses, which risk inducing quenches. Based on experience at the LHC, the collimation efficiency is expected to be about two orders of magnitude worse than for protons [15], since heavy ions undergo nuclear fragmentation and electromagnetic dissociation (EMD) in the collimators. These processes produce secondary ion fragments with a charge-to-mass ratio different from the nominal one [15, 16]. They can emerge from the collimators within the geometric acceptance of the warm sections and pose a risk for the cold magnets in the DS, where the dispersion ramps up to the nominal value. For ion operation in the LHC, such DS losses limit the achievable intensity [17]. The purpose of this study is to evaluate the collimation cleaning performance for Pb ion beam operation in the HE-LHC.

SIMULATION SETUP

The simulations presented here are performed using the SixTrack-FLUKA active coupling framework [18], in which SixTrack [19–23] performs 6D symplectic tracking in the magnetic lattice and FLUKA [24, 25] provides a full Monte-Carlo simulation of physics interactions inside the collimators. Thanks to the addition of support for arbitrary ions species [26], this method provides predictions in good agreement with measurements of ion collimation efficiency [15, 27]. The lattice used to study the betatron

* This work was supported in part by the European Commission under the HORIZON2020 Integrating Activity project ARIES, grant agreement 730871; Science and Technology Facilities Council grant ST/N504269/1, ST/P00203X/1, ST/N001583/1

† andrey.abramov.2012@live.rhul.ac.uk

Table 1: Summary of Simulation Parameters

Parameter	Value
Optics Version	helhc_23x90_V0.4
β^*	10 m
Crossing angle	OFF
N_{bunches}	1248
$N_{\text{ions}}/\text{bunch}$	2.1×10^8
Particle	$^{208}\text{Pb}^{82+}$
Ion normalised emittance (ϵ_N)	$0.993 \mu\text{m}$
Equivalent proton normalised emittance (ϵ_{Np})	$2.5 \mu\text{m}$
Energy (E)	1107 TeV
Equivalent proton energy	13.5 TeV
Energy/Nucleon (E/N)	5.32 TeV
Estimated quench limit	$2 \times 10^{-4} \text{ m}^{-1}$
Impact parameter	$1 \mu\text{m}$

cleaning in the simulations is the HE-LHC version 0.4, with TCLDs included and using injection optics at top energy (13.5 Z TeV). The crossing angle does not affect the local cleaning efficiency in IR7 and it is set to 0 for simplicity. A summary of simulation parameters can be found in Table 1.

To make a first comparison between the simulated losses and the magnet quench limit, it is conservatively assumed that the HE-LHC magnets quench at a steady-state load of 10 mW cm^{-3} . This is based on studies for the FCC-hh, where similar magnets are used [28], and it is twice the limit assumed for LHC magnets at 7 TeV during the LHC design stage [29]. The allowed flux of impacting nucleons can then be estimated to $3.1 \times 10^6 \text{ nucleons m}^{-1}\text{s}^{-1}$ for HE-LHC at 13.5 Z TeV by scaling down the rate allowed at the LHC from Ref. [29] by the change in quench limit and the approximate increase in peak power density per nucleon as in Ref. [30]. This estimate could be improved through dedicated energy deposition studies. Assuming the HE-LHC baseline Pb beam parameters in Table 1 [31] and a minimum acceptable beam lifetime of 0.2 h, a limiting cleaning inefficiency of $2 \times 10^{-4} \text{ m}^{-1}$ is found for Pb ions. It should be noted that this number is possibly pessimistic, since recent studies of the quench limit of the HL-LHC 11T dipoles, made with similar Nb₃Sn technology as the HE-LHC magnets, have revealed significantly higher values [32]. This gives a safety margin on the results.

In a first study, the impact parameter of the ions impacting the primary collimator was varied, and it was found that the impact parameter listed in Table 1 results in the worst losses in the DS and hence this value is chosen for the simulations presented. The collimator openings in σ and mm are both taken from the corresponding proton case and the assumed Pb normalised emittance is adjusted accordingly. A summary of collimator settings can be found in Table. 2. The physical opening of the horizontal TCP is 0.81 mm and the TCLD openings are set at 1.17 mm (cell 8) and 1.57 mm (cell 10). For the results presented, 1.5 million primary Pb ions were tracked for up to 700 turns.

Table 2: Summary of Collimator Settings. See Tab. 1 for emittance settings. The materials are carbon-fibre composite (CFC) and tungsten alloy (Inermet180).

Collimator	Opening [σ]	Count	Material
IR7 TCP	6.7	3	CFC
IR7 TCSG	9.1	11	CFC
IR7 TCLA	11.5	5	Inermet180
TCLD cell 8	18.1	1	Inermet180
TCLD cell 10	22.2	1	Inermet180
IR3 TCP	17.7	1	CFC
IR3 TCSG	21.3	4	CFC
IR3 TCLA	23.0	4	Inermet180

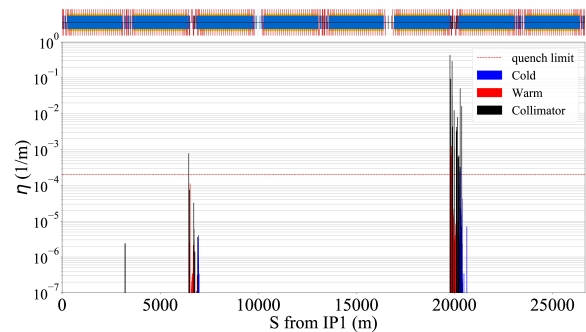


Figure 1: Loss map of the whole HE-LHC ring. The magnetic lattice elements are depicted on top.

RESULTS

As an example of the results, the simulated betatron loss map in the horizontal plane is shown in Fig. 1 and a zoom in IR7 is shown in Fig. 2. It can be observed that almost no losses leak out of the collimation insertions IR3 (momentum cleaning, at $S \approx 6 \text{ km}$) and IR7 (for betatron cleaning, at $S \approx 20 \text{ km}$) to cold magnets around the ring, which is a very promising result. Almost all ion fragments are successfully cleaned by the TCLDs. No significant losses are observed in the arcs or the experimental insertions. The only sections of the machine that suffer cold losses are the dispersion suppressors of the collimation insertions. While the losses in the DS of IR3 are tolerable, there are two clusters of losses in the DS of IR7 with a magnitude up to 50% above the assumed quench limit as seen in Fig. 2. One of the loss clusters occurs immediately upstream of the TCLD in cell 8 and the other one immediately downstream. To fully assess the risk of quenches from these losses, a local energy deposition study should be carried out, including the full shower development. The situation could possibly improve if further magnet studies are performed, which could potentially allow an increased quench level estimate. Nevertheless, the observed losses could be a concern and therefore these losses are analysed in detail in the following before potential mitigation strategies are discussed.

The transverse distribution of aperture losses in the DS, shown in Fig. 3, demonstrates that most aperture impacts

Content from this work may be used under the terms of the CC BY 3.0 licence (© 2019). Any distribution of this work must maintain attribution to the author(s), title of the work, publisher, and DOI

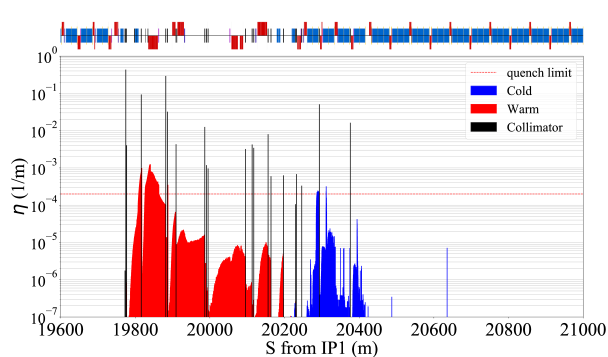


Figure 2: Zoom of the betatron collimation section in IR7 from Fig. 1. The magnetic lattice elements are depicted on top.

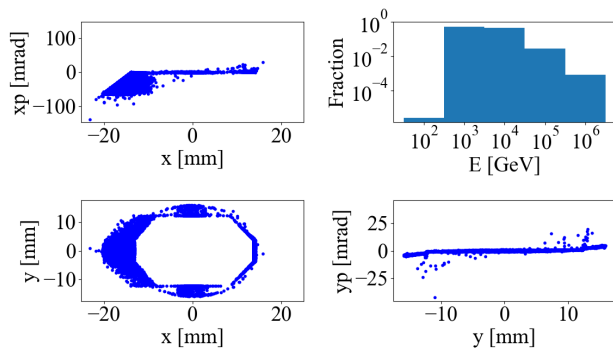


Figure 3: Transverse distribution of aperture losses in the DS ($S = 20250 - 20500$ m). Particles lost on collimators are not included in the plot. On the lower left plot, the outline of the nominal arc aperture profile can be observed.

occur on the inside of the ring, indicating predominantly lower magnetic rigidity of the particles lost there. More detailed analysis of the ion species and the collimator at which they originate is presented in Fig. 4. The heaviest fragments seen in the losses have $A = 203$, meaning that no nominal $^{208}\text{Pb}^{82+}$ ions or the heaviest EMD products, $^{207}\text{Pb}^{82+}$ and $^{206}\text{Pb}^{82+}$, are reaching the aperture in the DS. The TCLD collimator in cell 8 is successfully intercepting the heaviest fragments, but it is also generating a broad spectrum of shower products that reach the aperture. The loss cluster downstream of the TCLD that exceeds the quench limit is caused by secondary ions and protons out-scattered by the TCLD itself. The largest contribution to energy lost in the DS overall is given by light fragments coming from the horizontal TCP. These light fragments also dominate the large loss cluster immediately upstream of the TCLD.

There are several different methods under investigation for alleviating the DS losses. Since the losses are dominated by fragments that originate at the horizontal TCP and escape the warm section, optimisation of the openings of the TCGSs and the TCLAs is being studied. There is a possibility to tighten the collimator hierarchy in an attempt to intercept the losses, but it is necessary to carefully consider the hierarchy tolerances. Another option is to use an orbit bump

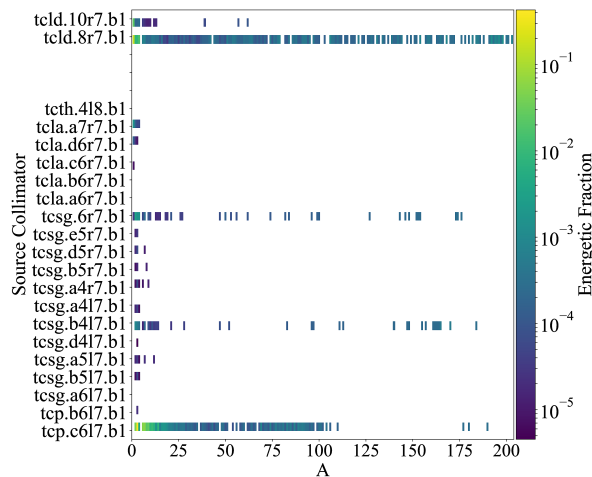


Figure 4: Source collimator and lost energy impact of ion species in the DS ($S = 20200 - 20500$ m). The energy fraction is with respect to the total energy lost on the aperture in the DS. Particles lost on collimators are not included in the plot.

towards the outside of the ring to push the losses upstream of the TCLD onto the collimator itself, similarly to what has been implemented in the LHC to alleviate losses due to secondary beams from Bound-Free Pair Production (BFPP) at experimental IPs by moving the losses to a more favourable location [33]. Furthermore, the option for a longer TCLD collimator will also be investigated, as well as local beam screen shielding.

CONCLUSION AND OUTLOOK

The first studies of collimation system performance for Pb ion beam operation in the HE-LHC have been carried out. For betatron collimation at top energy, the collimation system designed and optimised for protons was found to be generally very effective and almost no losses occur outside of the collimation insertions. In particular, the aperture of the arcs and the experimental insertions was not found to suffer any significant losses, in spite of the very challenging conditions with almost 50 MJ of stored beam energy and a much lower cleaning efficiency than for proton beams. The only part of the ring that sustains notable cold losses was observed to be the DS of the betatron collimation insertion. Two large loss clusters on either side of a TCLD collimator in cell 8 have been identified with magnitudes exceeding estimated quench limit by up to 50%. The upstream cluster is found to be dominated by light fragments originating in the horizontal TCP, while the peak of the downstream cluster results from secondary ion fragments and protons out-scattered by the TCLD collimator itself. A comprehensive energy deposition study is needed to fully evaluate the quench risk from those losses. An investigation of mitigation strategies that can reduce the losses is currently ongoing with a tighter collimation hierarchy, an orbit bump, and a longer TCLD collimator being considered.

REFERENCES

- [1] F. Zimmermann *et al.*, “High-Energy LHC Design”, in *Proc. 9th Int. Particle Accelerator Conf. (IPAC’18)*, Vancouver, Canada, Apr.-May 2018, pp. 269–272. doi:10.18429/JACoW-IPAC2018-MOPMF064
- [2] M. Benedikt, “Status of the Future Circular Collider Study”, in *Proc. 25th Russian Particle Accelerator Conf. (RuPAC’16)*, Saint Petersburg, Russia, Nov. 2016, pp. 34–38. doi:10.18429/JACoW-RUPAC2016-TUYMH01
- [3] F. Zimmermann, “High energy large hadron collider conceptual design report”, to be published, tech. rep., 2018.
- [4] M. Benedikt *et al.*, “Future circular collider,” *CERN-ACC-2018-0058*, Dec 2018.
- [5] R. Bruce, *et al.*, “Reaching record-low β^* at the CERN Large Hadron Collider using a novel scheme of collimator settings and optics,” *Nucl. Instrum. Methods Phys. Res. A*, vol. 848, pp. 19 – 30, Jan 2017.
- [6] R. Bruce, *et al.*, “Sources of machine-induced background in the ATLAS and CMS detectors at the CERN Large Hadron Collider,” *Nucl. Instrum. Methods Phys. Res. A*, vol. 729, pp. 825 – 840, 2013.
- [7] R. Bruce, *et al.*, “Collimation-induced experimental background studies at the CERN Large Hadron Collider,” *Phys. Rev. Accel. Beams*, vol. 22, p. 021004, Feb 2019.
- [8] R. W. Assmann *et al.*, “The Final Collimation System for the LHC”, in *Proc. 10th European Particle Accelerator Conf. (EPAC’06)*, Edinburgh, UK, Jun. 2006, paper TUODFI01, pp. 986–988.
- [9] S. Redaelli, “Beam cleaning and collimation systems“, *CERN Yellow Report CERN-2016-002*, vol. 2, pp. 403–407, 2016.
- [10] G. Apollinari, *et al.* (editors), *High-Luminosity Large Hadron Collider (HL-LHC): Technical Design Report V. 0.1*. CERN Yellow Reports: Monographs. CERN-2017-007-M, Geneva: CERN, 2017.
- [11] S. Redaelli *et al.*, “Collimation upgrades for HL-LHC”, in *Proc. LHC Performance Workshop, Chamonix*, France, Sep. 2014, pp. 225–231. 10.5170/CERN-2015-002
- [12] R. Bruce, A. Marsili, and S. Redaelli, “Cleaning Performance with 11T Dipoles and Local Dispersion Suppressor Collimation at the LHC”, in *Proc. 5th Int. Particle Accelerator Conf. (IPAC’14)*, Dresden, Germany, Jun. 2014, pp. 170–173. doi:10.18429/JACoW-IPAC2014-MOPRO042
- [13] T. Risselada, “Survey offsets, IR3 & 7 layouts, DS changes for TCLDs,” *Presentation at 35th HE-LHC design meeting, CERN, Geneva Switzerland*, 2018. <https://indico.cern.ch/event/774203>
- [14] J. M. Jowett *et al.*, “The 2018 Heavy-Ion Run of the LHC”, presented at the 10th Int. Particle Accelerator Conf. (IPAC’19), Melbourne, Australia, May 2019, paper WEYY-PLM2, this conference.
- [15] P. Hermes, *et al.*, “Measured and simulated heavy-ion beam loss patterns at the CERN Large Hadron Collider,” *Nucl. Instrum. Methods Phys. Res. A*, vol. 819, pp. 73 – 83, Feb 2016.
- [16] P. Hermes, *Heavy-Ion Collimation at the Large Hadron Collider: Simulations and Measurements*. PhD thesis, University of Munster, CERN-THESIS-2016-230, 2016.
- [17] P. Hermes, *et al.*, “LHC Heavy-Ion Collimation Quench Test at 6.37Z TeV,” *CERN-ACC-NOTE-2016-0031*, Mar 2016.
- [18] A. Mereghetti *et al.*, “SixTrack-Fluka Active Coupling for the Upgrade of the SPS Scrapers”, in *Proc. 4th Int. Particle Accelerator Conf. (IPAC’13)*, Shanghai, China, May 2013, paper WEPEA064, pp. 2657–2659.
- [19] F. Schmidt, “SixTrack. User’s Reference Manual,” *CERN/SL/94-56-AP*, 1994.
- [20] G. Robert-Demolaize *et al.*, “A new version of sixtrack with collimation and aperture interface”, in *Proc. Particle Accelerator Conf. (PAC’05)*, Knoxville, USA, May 2005, paper FPAT081, pp. 4084–4086.
- [21] “SixTrack web site.” <http://sixtrack.web.cern.ch/SixTrack/>
- [22] R. Bruce *et al.*, “Simulations and measurements of beam loss patterns at the CERN Large Hadron Collider,” *Phys. Rev. ST Accel. Beams*, vol. 17, p. 081004, Aug 2014.
- [23] P. Hermes *et al.*, “Simulation Tools for Heavy-Ion Tracking and Collimation”, in *Proc. ICFA Mini-Workshop on Tracking for Collimation in Particle Accelerators*, CERN, Geneva, Switzerland, 2015, CERN-2018-011-CP, pp. 73–88.
- [24] A. Ferrari *et al.*, “FLUKA: a multi-particle transport code,” *CERN Report CERN-2005-10*, 2005.
- [25] T. Bohlen *et al.*, “The FLUKA code: Developments and challenges for high energy and medical applications,” *Nuclear Data Sheets*, no. 120, pp. 211–214, 2014.
- [26] P. D. Hermes, R. Bruce, and R. De Maria, “Symplectic Tracking of Multi-Isotopic Heavy-Ion Beams in SixTrack”, in *Proc. 7th Int. Particle Accelerator Conf. (IPAC’16)*, Busan, Korea, May 2016, pp. 1450–1453. doi:10.18429/JACoW-IPAC2016-TUPMW015
- [27] P. D. Hermes *et al.*, “Simulation of Heavy-Ion Beam Losses with the SixTrack-FLUKA Active Coupling”, in *Proc. 7th Int. Particle Accelerator Conf. (IPAC’16)*, Busan, Korea, May 2016, pp. 2490–2493. doi:10.18429/JACoW-IPAC2016-WEPMW029
- [28] R. Bruce *et al.*, “Collimation system studies for the FCC-hh”, presented at the 10th Int. Particle Accelerator Conf. (IPAC’19), Melbourne, Australia, May 2019, paper MOPRB048, this conference.
- [29] J. B. Jeanneret *et al.*, “Quench levels and transient beam losses in LHC magnets,” *LHC Project Report 44*, CERN, 1996.
- [30] D. Schulte, “FCC-hh machine layout and optics,” *Presentation at the FCC 2016 week, Rome, Italy*, 2016. <https://indico.cern.ch/event/438866>
- [31] E. N. Shaposhnikova *et al.*, “LHC Injectors Upgrade (LIU) Project at CERN”, in *Proc. 7th Int. Particle Accelerator Conf. (IPAC’16)*, Busan, Korea, May 2016, pp. 992–995. doi:10.18429/JACoW-IPAC2016-MOPOY059
- [32] L. Bottura *et al.*, “Expected performance of 11T and MB dipoles considering the cooling performance,” *Presentation at 8th HL-LHC collaboration meeting, CERN, Geneva Switzerland*, 2018. <https://indico.cern.ch/event/742082/sessions/282742>
- [33] R. Bruce *et al.*, “Beam losses from ultraperipheral nuclear collisions between Pb ions in the Large Hadron Collider and their alleviation,” *Phys. Rev. ST Accel. Beams*, vol. 12, p. 071002, Jul 2009.